Azerbaijan Journal of Physics

Fizika

GROWTH AND OPTICAL PROPERTIES OF Cu(In,Ga)Se₂ THIN FILMS ON FLEXIBLE METALLIC FOILS

A.V. MUDRYI, A.V. KOROTKI, V.F. GREMENOK, E.P. ZARETSKAYA,

State Scientific and Production Association "Scientific-Practical Materials Research Centre of the National Academy of Sciences of Belarus , P. Brovka str. 19, 220072 Minsk, Belarus, email: gremenok@ifttp.bas-net.by

V.B. ZALESSKI

Institute of Electronics, National Academy of Sciences of Belarus, 220090, Logoiski trakt 22, 220090 Minsk, Belarus, email: zalesski@inel.bas-net.by

N.N. MURSAKULOV, N.N.ABDULZADE, Ch.E.SABZALIYEVA

Institute of Physics, National Academy of Azerbaijan, H. Cavid ave., 33, Baku, Az-1143, email: nmursakulov@physics.ab.az

Polycrystalline Cu(In,Ga)Se₂ (CIGS) thin films on flexible metallic foils were prepared by two-stage selenization of sputter-deposited Cu- Ga- In precursors. The phases, surface morphologies, microstructures and elemental depth profiles of the CIGS films prepared on different metallic flexible foils (titanium, molybdenum, aluminum and stainless steel) were analyzed. To characterize the structure quality and intrinsic defect nature low-temperature (4.2 – 300 K) photoluminescence (PL), photoluminescence excitation (PLE) and optical transmission measurements were performed. Experiments show that the structural and optical properties of CIGS absorber layers strongly depend on the growth condition, chemical composition and type of the substrate. The band gap energy (E_g) of CIGS chalcopyrite compounds, grown on nontransparent flexible metallic substrates was estimated from PLE data. Excitation power and temperature dependent PL measurements shows that the broad bands in the near-band edge spectral region are caused by the band-tail recombination.

1. INTRODUCTION

The chalcopyrite semiconductor Cu(In,Ga)Se₂ (CIGS) thin-film cells have demonstrated the highest efficiency on the laboratory and industrial scale. The conversion efficiency approaching the theoretical value of over 20 % are already reached for CIGS thin-film solar cells on glass substrates [1,2]. In the last years an increasing number of the studies have been performed on the CIGS thin films fabricated on ultralightweight flexible metallic foils and polymer substrates [3-5]. The use of flexible substrates instead of the commonly used rigid soda lime glasses offers new possibilities for the application of solar cells in space and terrestrial photovoltaic power system. Conversion efficiencies up to 16 – 17.5 % have achieved for the CIGS solar cells on flexible metallic substrates [6].

In this paper we report new results on a study of physical properties (structural, morphological and optical) of CIGS thin films grown on different flexible metallic foils (titanium, molybdenum, aluminum, stainless steal). To study the intrinsic defect nature detailed low-temperature (4.2 – 300 K) PL and PLE measurements of CIGS thin films were performed.

2. EXPERIMENTAL

The CIGS films with thickness about of 1 – 2.5 μm were grown on thin metallic foils by DC magnetron sputtering of the Cu-In-Ga metallic alloys with subsequent two-stage selenization. In the first stage the precursor layers were heated for 10 min to temperature of 260 °C, and the initial reaction period for all selenization processes was maintained at 20 min. The selenization was completed by second recrystallization step (T_s) under temperatures 400 – 520 °C for ~ 20 – 60 min. The CIGS films with the same chemical composition were also prepared on soda lime glasses at the time for comparison.

The films surface morphology and microstructure were analyzed by scanning electron microscopy (SEM)

using JEOL 6400 SEM apparatus. The chemical composition and the depth profiling were determined by energy dispersive X-ray (EDX) analysis using a CAMEC SX-100 and Auger electron spectroscopy (AES) with simultaneous sputter etching using a Perkin Elmer Physics Electronic 590 model apparatus. The crystalline structure of the layers was studied by the X-ray diffraction (XRD) using a Siemens D5000 diffractometer with CuK₀ (λ = 1.5418 Å) radiation. The optical parameters of the reference CIGS thin films deposited onto Corning glass substrates were determined from transmittance (T) and reflection (R) measurements in the spectral range of 200 – 3000 nm at room temperature using a Carry 500 Scan UV-Vis-NIR spectrophotometer (Varian, USA). The PL spectra were analyzed using a 0.6 m diffraction monochromator. A liquid nitrogen cooled InGaAs p-i-n detector (Hamamatsu, Japan) was used for the PL signal detection. Signal amplification was based on lock in technique. For excitation, the 488 line of the Ar ion laser was used in the PL experiments. The samples were immersed into liquid nitrogen or helium during the measurements of the PL at 78 are 4.2 K, respectively. Temperature dependent measurements from 4.2 to 300 K were carried out in an evaporation cryostat equipped with suitable heaters and temperature sensors. The PLE spectra were measured using a 400 W halogen tungsten lamp combined with a grating monochromator (1200 groves mm⁻¹, focal length of 0.3 m) as an excitation source.

3. RESULTS AND DISCUSSION

The aim of these investigations was to develop a reproducible process of CIGS thin films deposition on different metallic foils for solar cells applications. Table 1 presents the average values of Cu, In, Ga and Se amounts determined by AES method for the all investigated films on metallic foils. The same elemental composition (Cu:In:Ga:Se in atomic %) in near-surface

region of CIGS films has been confirmed by EDX method. The chemical composition was determined by averaging the values from 5 different points on the surface of the same film.

Table 1. Chemical composition of CIGS thin films deposited on different metallic substrates (selenization temperature was maintained at 520 °C for 20 min)

Sample notation	Type substrate	Cu, at %	In, at %	Ga, at %	Se, at %
2X118	glass	26.2	24.8	1.9	46.7
1MX	Mo	29.1	22.2	3.3	45.4
2TX	Ti	24.1	26.1	2.2	47.6
1TMX	Ti with Mo layer	25.0	23.4	2.0	49.6
1HCMX	stainless steel with Mo layer	26.7	21.9	2.5	48.9
1AlDX	Al	21.7	26.0	2.2	50.1
1AlMX	Al with Mo layer	35.4	22.8	2.1	39.7

The AES spectra of CIGS thin films were analyzed over a range of kinetic energies from 100 to 1400 eV, using the primary electron beam of energy 5 keV. An example of these spectra, taken with a magnification of 1000 x, equivalent to an area of 100x100 μm^2 is shown in Fig. 1. This spectrum showed the presence of the following chemical elements: indium at 298, 345 and 408 eV; copper at 775, 848 and 921 eV; gallium at 1010 eV; selenium at 1193, 1205, 1237, 1312

and 1352 eV. The elemental composition at the surface was calculated from the relative intensity of the peak in the AES spectra and to be as follows: copper 30 at %, indium 21 at %, gallium 3 at % and selenium 46 at %. The chemical composition analyzed by EDX gives the same average atomic concentration (5 point on the surface of films).

The AES depth profile measurements were used to study the element distribution in the bulk of CIGS films. The chemical composition was obtained by sputtering on area with dimension approximate by of 100x100 μm^2 with energetic argon ions at a rate 500 Å/min or 1000 Å/min. The typical depth profile for 1MX sample obtained at optimal selenization conditions (T$_s$ – 520 °C, t = 20 min) is shown in Fig. 2. The depth profile presented in Fig. 2 is from the surface up to molybdenum foil. As observed, Cu, In, Ga and Se atomic concentrations remained fairly uniform through the depth of the CIGS films during 8 min of the sputtering process.

Further copper and indium concentration decreased rapidly. Ga concentration remained constant during the 6 min of the sputtering process, and then slightly increased. It is clear seen from Fig. 1 that Mo atomic concentration is sharply increased after initial stage of sputtering (8 min). The irregular distribution of elements Cu, In and Mo in the bordering to Mo-substrate region indicates formation of two-phase material MoSe$_2$ and CIGS in the bottom of the layer and agrees with XRD data and SEM image.

The AES measurement for other CIGS thin films (see Table 1) showed the uniform distribution of elements Cu, In, Ga and Se through the depth of the layers withought the formation additional phases in material that

agrees with the XRD data. The inhomogeneous elemental distribution was found only near interface between CIGS layers and corresponding metallic foils.
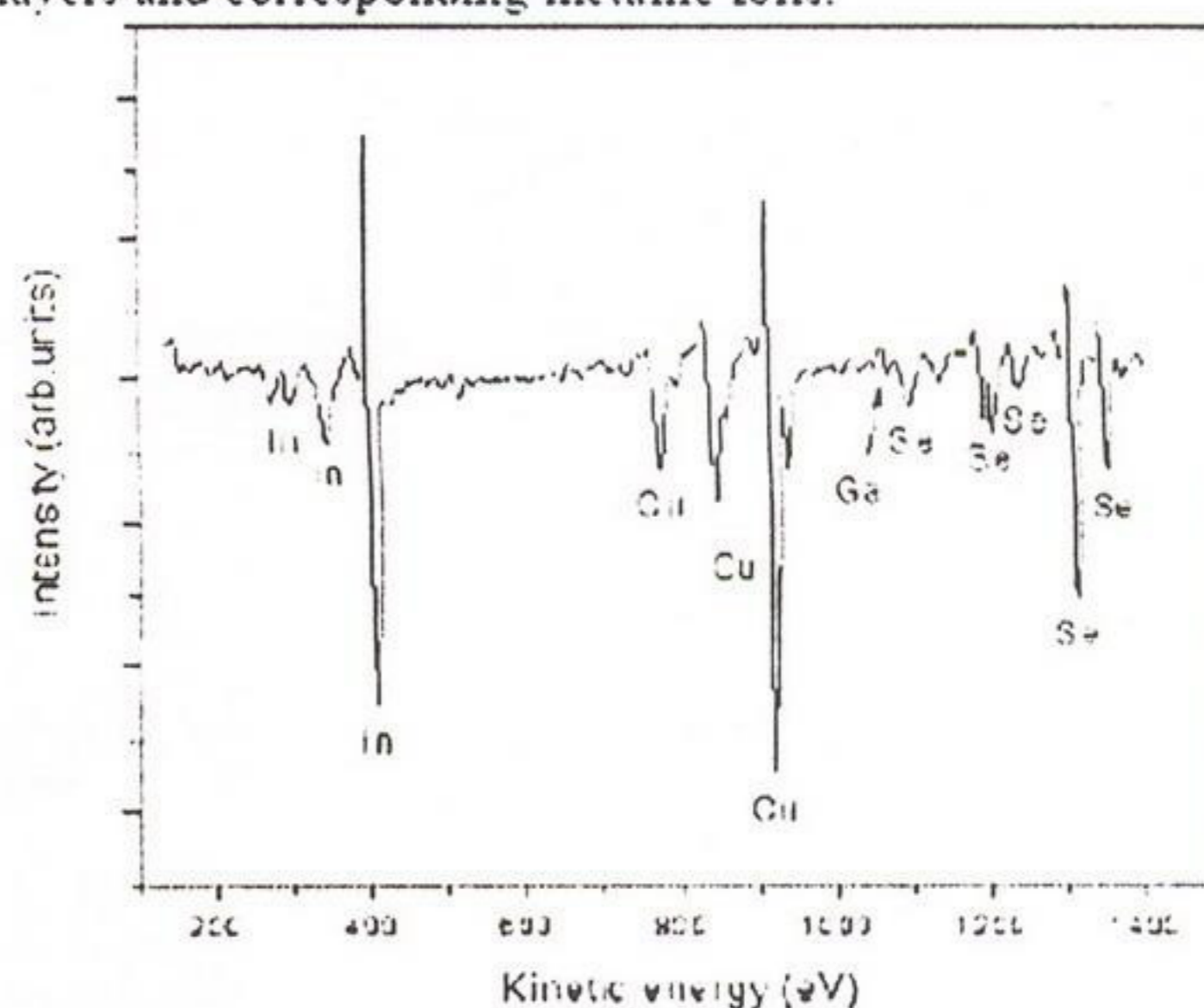

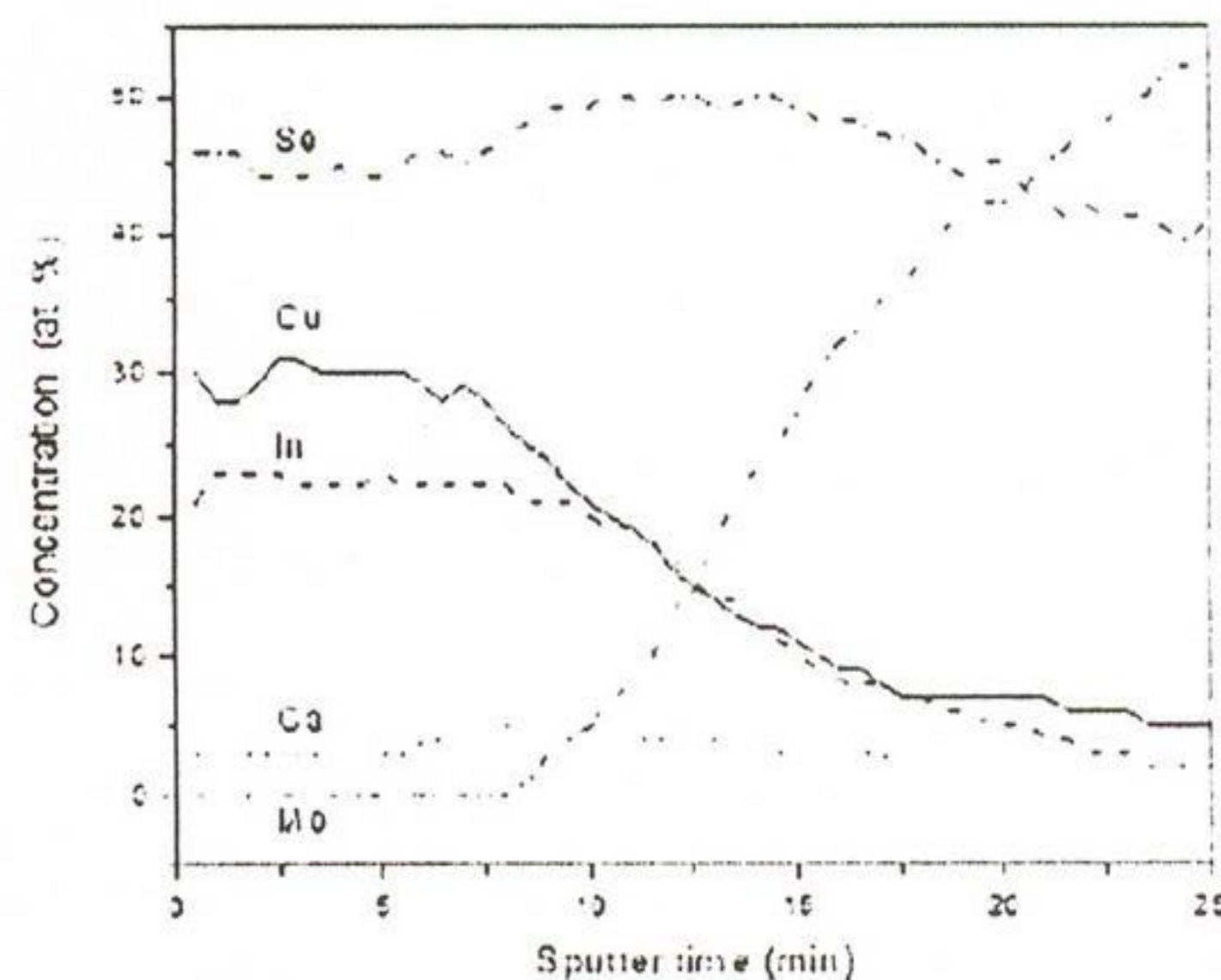Fig. 1 A typical AES spectrum of the CIGS film (sample 2X118)

Fig. 2 A AES depth profile of CIGS films on Mo foil (sample 2X118)

The phase formation and structure of CIGS thin films were characterized by X-ray diffraction. Fig. 3 show XRD pattern of structure – molybdenum foil/chalcopyrite semiconductor absorbing layer (sample 1MX). The observed phases in XRD pattern were identified by comparing the d-spacing with Joint Committee on Power Diffraction Standard (JCPDS) data files. The intense peak at 2Θ ≈ 58.63° and weak peak at 2Θ = 73.6 ° were from Mo foil, reflection (200) and (211), respectively, (JCPDS card 42-1120), that agrees with XRD data for similar structures [7]. The XRD pattern indicate the formation of two-phase material – MoSe$_2$ and CIGS. It was found that both of the materials MoSe$_2$ and CIGS are polycrystalline in nature. In the Fig. 3, the peaks at 2Θ ≈ 55.9° belong to the MoSe$_2$ phase (JCPDS card 72 – 1420). The XRD pattern also contains main reflections of CIGS phase such as (101), (112), (103), (211), (204)/(220), (116)/(312), (008)/(400), (316)/(332), (228)/(424). The strongest peak for chalcopyrite semiconductor compound CIGS was from the (112)

plane. indicating that the layer have preferred orientation towards to [112] direction.
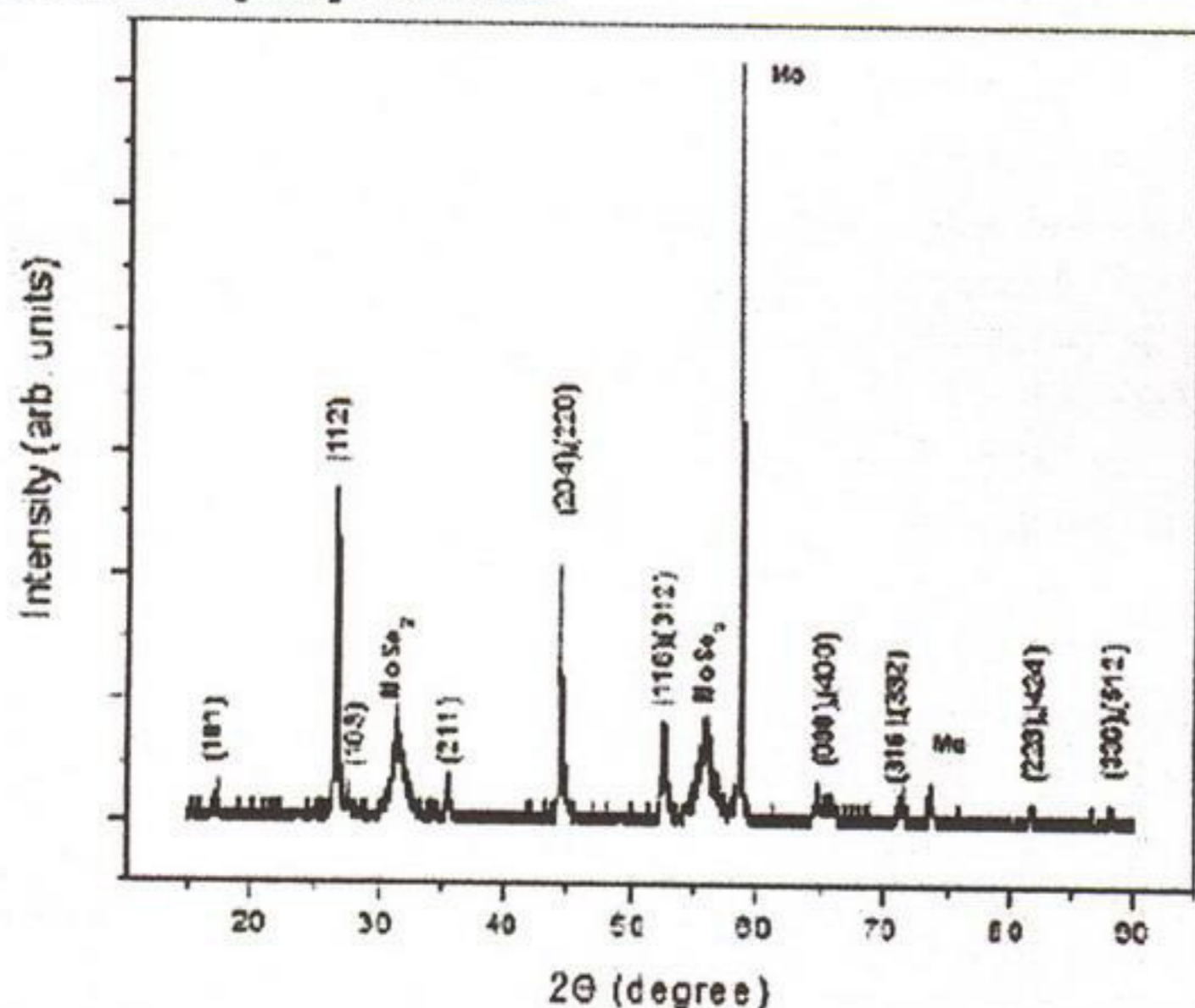

*Fig.3* X-ray diffraction spectra for a CIGS thin films on Mo foil (sample 2X118)

It was found that the degree of preferred orientation, evaluated from the intensity ratio $I_{112}/I_{204/220}$ to be ~ 1.4. It is shown that in the case of random orientation this ratio should be ~ 5 [8]. Lower value of $I_{112}/I_{204/220}$ for 1 MX film shows a poor degree of (112) preferred orientation. However, the degree of preferred orientation for 1MX film is increased from 1.1 to 1.4 with increasing of selenization temperature from 400 to 520 °C, respectively. XRD patterns of other samples (see Table 1) show characteristic diffraction peaks that can be also index on the basis of the tetragonal chalcopyrite structure CIS. All patterns showed a dominant (112) reflection and two weaker double reflections 204/220 and 116/132. The degree of preferential orientation of these films varies from 1.5 to 4. The diffraction peak (112) is strong in all patterns and becomes more dominant with increasing selenization temperature from 400 to 520 °C. No other phases were found for all CIGS thin films indicated in Table 1, excluded 1MX sample.

The surface morphology of CIGS thin films grown on metallic foils was found to be strongly dependent on the deposition condition and selenization temperature. The surface SEM micrograph of 1MX sample is shown in Fig.4. SEM image showed large, well-faceted dense grain structure and grain size to be about ~ 1-2.5 μm, i.e. comparable to the film thickness. It was also found from the SEM micrographs that the uniformity and adhesions of the films on different metallic foils improved with increasing of selenization temperature from 400 to 520 °C. The presence of the MoSe₂ sublayer (additional phase) the interface region it is clear seen from Fig. 4. SEM surface micrographs for other samples (Table 1) revealed structure that changed in density and grain sizes ~ 0.3 – 2.5 μm in dependence of selenization temperature and type of metallic substrate. Our investigations show that CIGS thin films with remarkable structural quality can be prepared by two-stage selenization method with different morphology ranging from polycrystalline to continuous single-crystalline depending on the selenization temperature and time of annealing. However, we observe

that CIGS films are not always as dense as shown in Fig. 4. In some cases the layer can become porous.

a
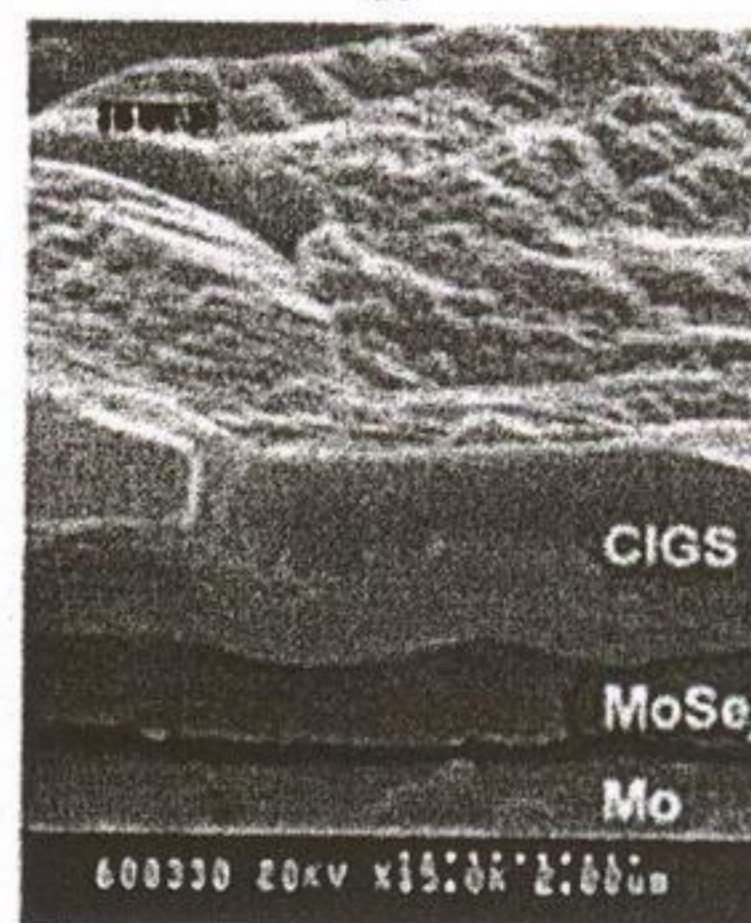
b
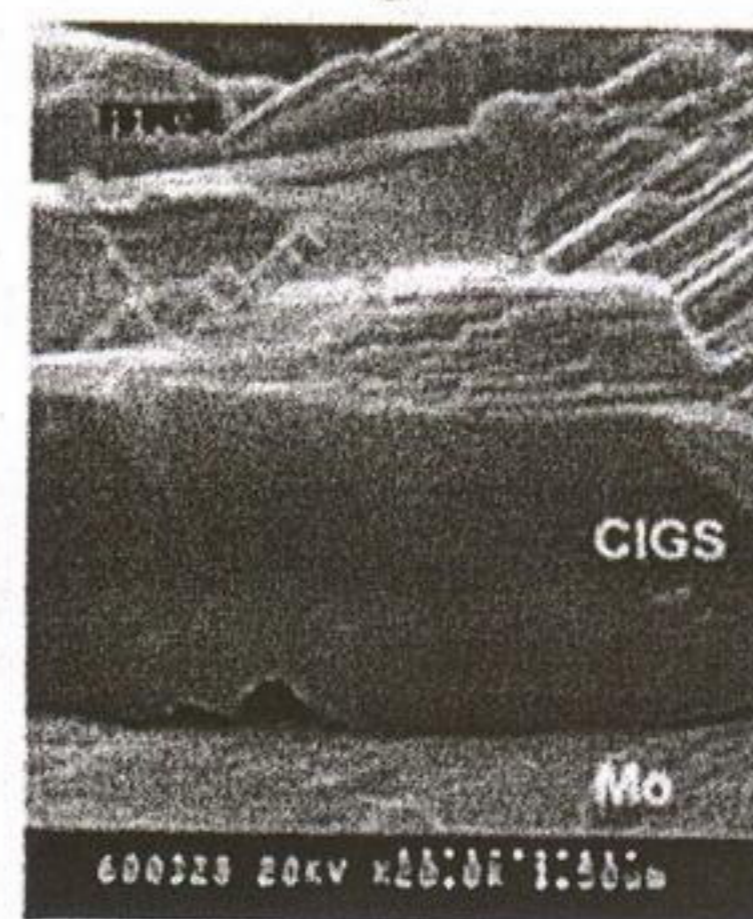
c

Fig.4 SEM micrographs of CIGS of CIGS films on Mo foil (sample 2X118): (a) – plane view; (b), (c) – cross-section image of a different parts of film with and without MoSe₂ sublayer, respectively

The optical properties of reference CIGS thin films on glass substrate were studied by measuring both transmittance (T) and reflection (R) spectra. Fig. 5a shows the T spectrum taken at room temperature. Sample 2X118 exhibit transparency ~ 35 - 45% in near-infrared region and has relatively sharp edge of an intrinsic absorption. The absorption coefficient of the film has been calculated using both optical transmission and reflection data and following relation [9]:

410

$$\alpha = -\frac{1}{d}\ln\frac{\sqrt{(1-R)^4 + 4T^2R^2} + (1-R)^2}{2T}, \quad (1)$$

where α is the absorption coefficient, d is the thickness of the film, T and R are the transmission and reflection, respectively. The reflectivity R was measured in the photon energy region of 1 - 2.5 eV and to be ~ 0.21 for 2X118 sample. In the case of allowed direct transitions the absorption coefficient is written as a function of the incident photon energy hv using the following equation [10]:

$$\alpha = A(hv - E_g)^{\frac{1}{2}} \quad (2)$$

were E_g and A are the optical band gap and a constant, respectively. The optical bang gap of the CIGS film was determined by extrapolating of the linear part of the spectral dependence $\alpha^2 \sim f(hv)$ to the photon energy axis, Fig. 5b. The E_g value determined from transmittance measurements to be ~ 1.06 eV for 2X118 sample.
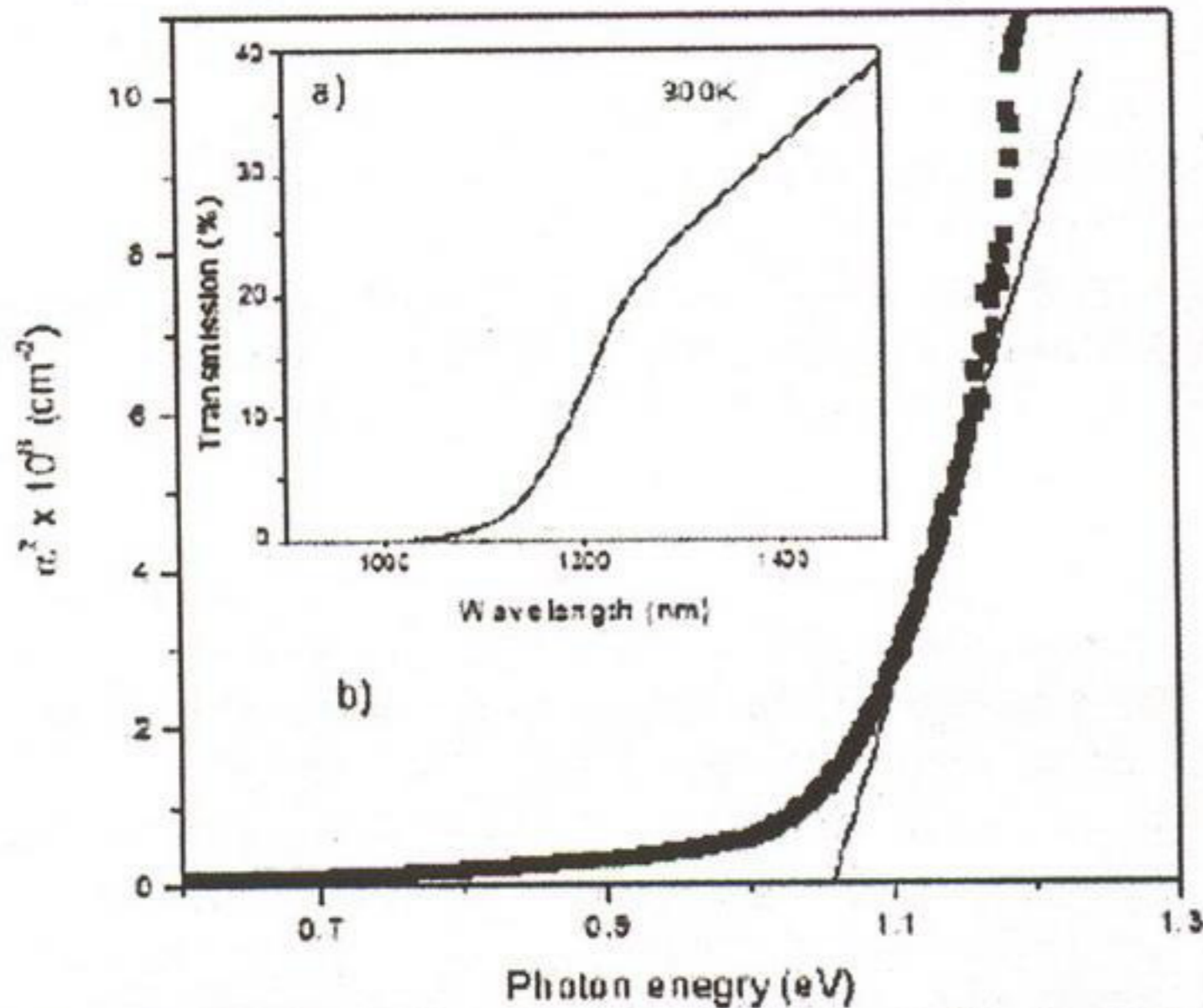

Fig. 5. Transmittance (a) and the dependence of α^2 vs hv (b) for CIGS film on glass substrate (sample 2X118).

A typical PL spectra of CIGS films at 4.2, 78 and 300 K are shown in Fig. 6. The single brood band at 1.03 with full-width at half-maximum intensity (FWHM) ~ 80 meV dominates the spectrum from 1MX sample at 4.2 K. It can be seen that broad band has an asymmetric spectral shape with a longer tail towards lower energies. This band shifts to a higher energy with increasing temperature as seen in the normalized PL spectra in Fig. 6b. This significant temperature shift can not be attributed to the band gap variation since the experimentally observed increase up to around 80 – 100 K is only about of 1.5 – 2 meV [11,12]. The FWHM and shape of a broad band change also upon increasing the temperature. The PL band become more symmetrical and it's FWHM slightly increase from 4.2 to 300 K. The single bands with similar temperature effects were also found in the PL spectra of other CIGS samples which composition a given in Table 1, see as an example Fig. 6. In order to identify the origin of the broad bands the excitation power dependence of the PL bands have been carried out. The excitation density

dependence of the PL bands is known to usually give an indication of the type of a recombination process involved. As an example Fig.7 shows the dependence of the broad bands energy position on excitation power at 4.2 K for three different levels of excitation density – 1 W·cm^{-2}, 5 W·cm^{-2} and 100 W·cm^{-2}. It is clear seen that increasing excitation intensity generate a significant high-energy shift of the bands (blue j-shift). The experiments show that j-shift has a different value and strongly depend on chemical composition and structural quality of CIGS films, Table 1. The shift increases for our samples from 2 to 18 meV per decade of change in excitation density.
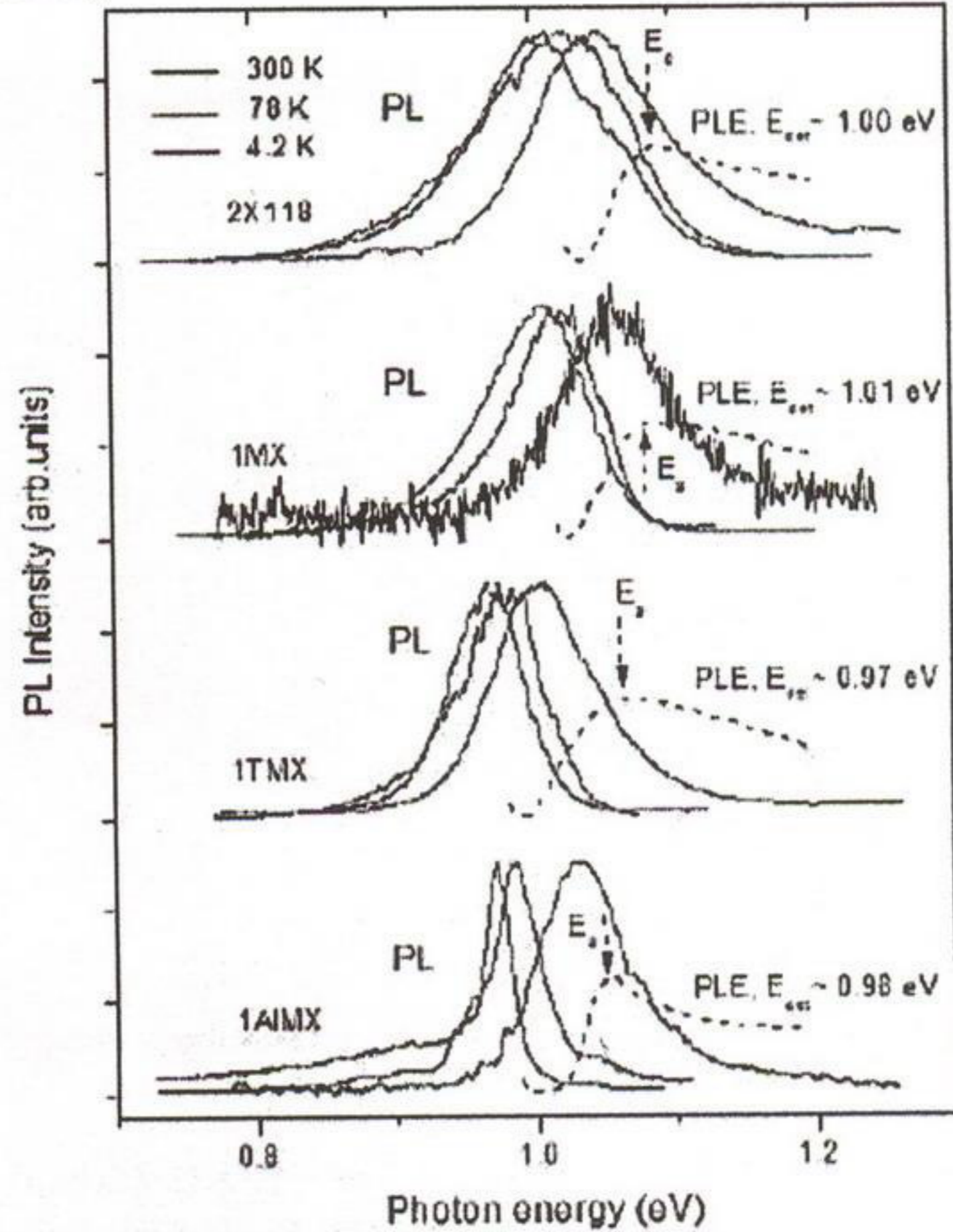

Fig.6 PL spectra of CIGS films taken at different temperatures 4.2, 78 and 300 K and PLE spectra taken at 78K.

Such large blue shift is in contradiction with donor-acceptor pair (DAP) recombination process. Usually the moderate shift-rate of 2 meV /decade of excitation density are characterized for donor-acceptor pair recombination in semiconductors [13,14]. Our experimental results may be consistently explained in the framework of the model of fluctuating potentials in highly doped and compensated semiconductors introduced by Shklovskii and Efros [15]. The statistically distributed potential fluctuations are due to high concentration of charged donors, acceptor and other defects. The spatial fluctuations in CIGS films cause fluctuations of the band gap energy and widening of the impurities levels within the forbidden gap of material and so-called band tails are formed [16,17]. The strong blue shift of the PL bands with increasing excitation density and temperature are due to changes of the carrier distribution in the energy levels of band tails. The amplitude of potential fluctuations strongly depends of the level defect concentration and degree of

compensation which are governed by the excess of (In+Ga) over Cu. This ratio determines the energy position of the band in PL spectra and j-shift magnitude [16,17]. More higher amplitude of potential fluctuation are induced the greater j-shift. As follows from Table 2 and Fig. 7 sample 1AlMX has more smaller j-shift for the main PL band at 0.97 eV.

Table 2. Chemical composition ratio and optical parameters of CIGS thin films (E_g values were determined from PLE measurements at 78 K)

Sample hotation	Composition ratio		E_g, eV	j-shift, meV/decade
	$\dfrac{Cu}{In + Ga}$	$\dfrac{Ga}{In + Ga}$		
2X118	0.99	0.07	1.08	15
1MX	1.14	0.13	1.08	18
2TX	0.85	0.08	1.05	13
1TMX	0.98	0.08	1.06	10
1HCMX	1.09	0.05	1.07	12
1AlDX	0.77	0.08	1.04	6
1AlMX	1.42	0.08	1.05	2

The dominant relatively narrow PL band at 0.97 eV has several low-energy phonon replica with an energy distance of $hw_{LO} \approx 29$ meV [18]. The narrow emission peak at 1.034 eV can also be found in a PL spectra of 1AlMX films. This peak caused by a bound exciton recombination [11,18]. Our earlier tentative identification indicate the relation of intense narrow band at 0.97 eV with the free-to-bound optical transitions, i.e. electron transitions to the acceptor levels (e-A-transitions) of Cu_{In} [18]. This analyzes leads us to conclude that 1AlMX is more structural and electronic perfect CIGS film among others, which were investigated. As an example Fig. 7 also compares PLE spectra of the broad bands for different samples. The PLE spectra were detected near the maxima of the corresponding broad bands, i.e. at E_{det}. as indicated in Fig. 7. As seen from PLE spectra the emission slightly grows reaching a maximum near gap energy E_g and than it slowly dropped forming structure less tails. In the most case the PL and PLE spectra are overlapped. This can be explained in the framework a model of fluctuating potentials. The bending of energy bands of semiconductor and the considerable increase in the density and depth of impurity band tails are occurs. The PL and PLE spectra are overlapped due to the absorption which extends to energies that are lower that the apparent band gap E_g (impurities tails). This experimental fact indicates that PLE spectra in the case of highly doped and compensated semiconductors, i.e. with fluctuating band edges, can be used only for an approximation determination of the corresponding bang gap E_g of semiconductor material. The PLE spectrum of 1AlMX sample exhibit a sharp edge and in this case the PL band the PLE tails do not overlap indicating more perfect quality of CIGS films. The value of the band gap E_g determined for such type of the PLE spectra in this case is more reliable and exact. More detailed consideration of these effects may be found in recent paper [19].

So, our investigations show that under optimized conditions of high-temperature stage selenization ($T_s \sim$ 500 – 520 °C, t ~ 20 min) single phase CIGS material with (112) preferred orientation can be grown. The chemical composition of films to be independent on the type of metallic foils but, as expected, strongly dependent on the composition and uniformity of the precursors as well as on the deposition conditions. It is also found that CIGS films have a strong adhesion to Mo, Al and stainless steel with the exception to Ti foil.
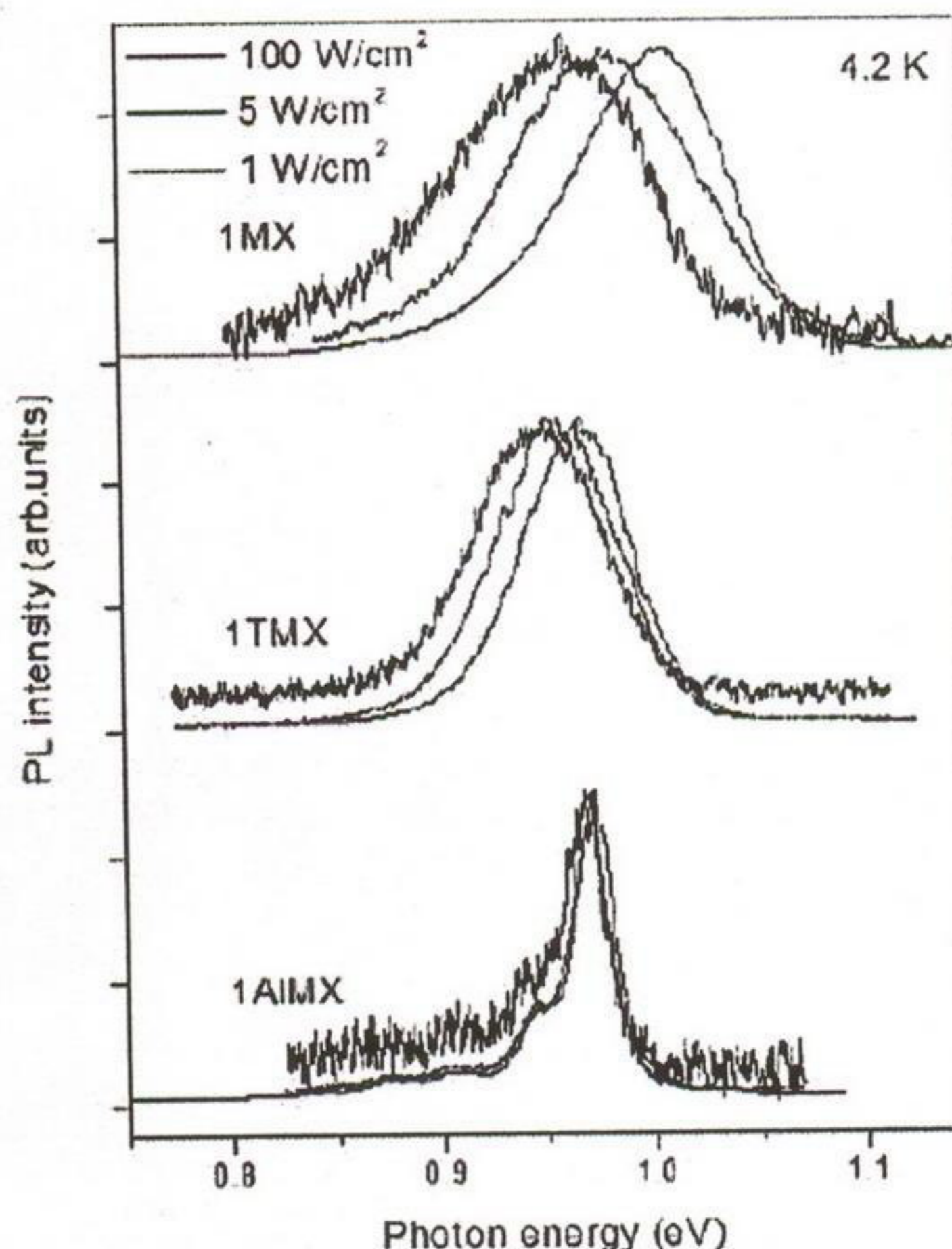

Fig.7 Excitation power dependence of PL spectra for different excitation densities.

4. CONCLUSIONS

Thin films of CIGS were grown by two-stage selenization of sequentially deposited Cu, Ga and In precursors. The precursors were deposited on flexible metallic foils by DC magnetron sputtering.. XRD, EDX and AES measurements revealed a near stoichiometric composition of the films for T_s not exceeding 520 °C. X-ray patterns showed preferred [112] orientation for all investigated CIGS film on different metallic foils (titanium, molybdenum, aluminum, stainless steel). Optical absorption measurements of the reference CIGS films on the glass substrate revealed value of E_g about of 1.06 eV. For the first time PLE measurements were employed to determine the band gap energy of CIGS film on nontransparent metallic substrates. It is found that the structural and optical properties of CIGS absorber layers are strongly depend on the growth condition, type of substrate and chemical composition. CIGS films of high structure and electronic quality were obtained with selenization at 520 °C for 20 min on Al foils.

[1]. *K. Ramanathan, M.A. Contreras, C.L. Perkins, S. Asher, F.S. Hasoon, J. Keane, D.L. Young, M. Romero, W. Metzger, R. Noafi, J. Ward, A. Dauda,* Prog. Photovolt. Res. Appl. 11 (2003) 225.

[2]. *M.A. Contreras, K. Ramanathan, J. AbuShama, F.S. Hasoon, D. L. Young, B. Egaas, , R. Noafi,* Prog. Photovolt. Res. Appl. 13 (2005) 209.

[3]. *N.G. Dhere, V.S. Gade, A.A. Kadam, A.H. Jahagirdar, S.S. Kulkarni, S.M. Bet* Mater. Sci. Engin. B 116 (2005) 303.

[4]. *F. Kessler, D. Herrmann, M. Powalla,* Thin Solid Films 480-481 (2005) 491.

[5]. *T. Satoh, Y. Hashimoto, S. Shimakawa, S. Hayashi, T. Negami,* Sol. Energy Mater. Sol. Cells 75 (2003) 65.

[6]. *F. Kessler, D. Rudmann,* Solar Energy 77 (2004) 685.

[7]. *J. Cowen, L. Lucas, F. Ernst, P. Pirouza, A. Heppb, S. Bailey,* Mater. Sci. Engin. B 116 (2005) 311.

[8]. *J. Muller, J. Nowoczin, H. Schmitt,* Thin Solid Films 496 (2006) 364.

[9]. *D.K.Schroder,* Semiconductor Material and Device Characterisation, Wiley, New York, 1990.

[10]. *J.I.Pankove,* Optical Processes in Semiconductors, Prentice Hall, Englewood, New York, 1971.

[11]. *A.V.Mudryi, M.V.Yakushev, R.D.Tomlinson, A.E.Hill, R.D.Pilkington, V.Bodnar, I.A.Victorov, V.F.Gremenok,* Appl. Phys. Lett. 77 (2000) 2542

[12]. *P.W.Yu,* J.Appl. Phys. 47 (1976) 677.

[13]. *S.Zott, K.Leo, M.Ruckh, H.W.Schock,* J. Appl. Phys. 82 (1997) 356.

[14]. *E.Zacks, A.Halperin,* Phys. Rev. B6 (1972) 3072.

[15]. *B.I.Shklovskii, A.L.Efros,* Electronic Properties of Doped Semiconductors. Springer Verlag, Berlin, 1984.

[16]. *I.Dirnstorfer, M.Wagner, D.M.Hofmann, M.D.Lampert, F.Karg, B.K.Meyer,* Phys. Status Solidi (a) 168 (1998) 163.

[17]. *J. Krustok, H.Collan, M.Yakushev, K.Hjelt,* Physica Scripta T79 (1999) 179.

[18]. *M.V.Yakushev, A.V.Mudryi, V.F.Gremenok, V.B.Zalesski, P.I.Romanov, Y.V.Feofanov, R.W.Martin, R.D.Tomlinson,* J. Phys. Chem. 64 (2003) 2005.

[19]. *S.Siebentritt, N.Papathanasiou, M.Lux-Steiner,* Phys. Status Solidi (b) 242 (2005) 2627.